PNAS
www.pnas.org

Supplementary Information for

A case of convergent evolution: several viral and bacterial pathogens hijack RSK kinases through a common linear motif.

Frédéric Sorgeloos, Michael Peeters, Yohei Hayashi, Fabian Borghese, Nicolas Capelli, Melissa Drappier, Teresa Cesaro, Didier Colau, Vincent Stroobant, Didier Vertommen, Grégory de Bodt, Stéphane Messe, Ignasi Forné, Felix Mueller-Planitz, Jean-François Collet, and Thomas Michiels

Email: thomas.michiels@uclouvain.be

This PDF file includes:

Supplementary Information Text

Extended Materials and Methods.

Cells

BHK-21 cells (ATCC) were cultured in Glasgow-minimal essential medium (Gibco) supplemented with 2.95 g/l of tryptose phosphate broth, 100 IU penicillin/ml, 100μg streptomycin/ml (Lonza) and 10% of newborn calf serum (BioWest). 293T (1), HeLa-M (2) and L929 cells (ATCC) were cultured in Dulbecco's modified Eagle medium (Lonza) supplemented with 10% foetal bovine serum (Sigma), 100 IU penicillin/ml and 100μg streptomycin/ml (Lonza). Cells were cultured at 37°C in a humidified atmosphere containing 5% CO2.

Plasmids, retroviral and lentiviral constructs

Expression plasmids and retro/lentiviral expression vectors are presented in Table S1. Plasmid vectors include pcDNA3 (Invitrogen) for mammalian expression, and pET-15b (Novagen) and pRSFDUET (Novagen) for bacterial expression. Plasmid pX461 (3) was used for CRISPR-Cas9 inactivation of RSK1 and RSK2 genes. pLKO.1 (4) derivatives, where the neomycin resistance gene was substituted for the puromycin resistance gene, were used to knock down RSK1 and RSK2 expression. Retroviral expression vectors were derived from pQCXIH (Clontech) and lentiviral vectors were derived from pTM952, a derivative of pCCLsin.PPT.hPGK.GFP.pre (5). Lentiviral constructs expressing human RSKs were constructed using the Gateway technology Invitrogen) from donor plasmids Hs.RPS6KA1, Hs.RPS6KA2, Hs.RPS6KA3 and Hs.RPS6KA6 kindly provided by Dominic Esposito through the Addgene collection (Addgene refs: 70573, 70575, 70577, and 70579, respectively). Except when otherwise indicated, vectors used for ectopic RSK2 expression expressed mouse RSK2, which differs from human RSK2 by a single aminoacid. Note that, where indicated, lentiviral or retroviral constructs were transfected as expression plasmids instead of being transduced.

Viruses

TMEV (6) and EMCV (7) derivatives were rescued by electroporation of BHK-21 cells with *in vitro* transcribed viral RNA from plasmids carrying the corresponding cDNAs. After completion of the cytopathic effect, usually between 48 and 72 h after transfection, culture supernatants were freeze-thawed and clarified lysates were stored in aliquots at -70°C. Viral titres were determined by standard plaque assay on BHK-21 cells.

Cell infection

Cells were washed in serum-free medium and infected at the indicated multiplicity of infection (MOI). One hour after virus addition, serum-containing medium was added to the cultures. Except when otherwise specified, L929 cells were infected for 8 hours and HeLa-M cells were infected for 12 hours before sample collection.

Cell transfection

293T cells were seeded the day before transfection using TransIT-LT1 (Mirus) with a DNA/transfection

reagent ratio of 1 μg / 3 μl, according to the manufacturer's instructions. Cells were harvested 24 hours after transfection.

Immunoprecipitations

Cells were lysed on ice in 50mM Tris-HCl pH8, 150mM NaCl, 0.5% NP40, 2mM EDTA 1mM PMSF and supplemented with protease/phosphatase inhibitors (Pierce). A sample (15 %) of the lysate was collected as control and mixed with Laemmli buffer. The lysate was then incubated twice with protein A/G magnetic beads at 4°C for 20 min to remove non-specifically bound proteins. Supernatant was incubated with anti-FLAG (Sigma) or anti-HA antibodies (Pierce) coupled to magnetic beads at 4°C for 2 hours. The pellet was then washed four times with lysis buffer and resuspended in Laemmli buffer so that it was concentrated 6 times compared to the lysate.

Peptide-mediated pull-down

As for immunoprecipitation, cells were lysed in 50 mM Tris-HCl pH8, 150 mM NaCl, 0.5% NP40, 2 mM EDTA, 1 mM PMSF and supplemented with protease and phosphatase inhibitors. After preclearing lysates with protein A/G magnetic beads, supernatants were incubated with biotinylated peptides at a concentration of 2 μM at 4°C for 2 hours. Samples were then incubated with magnetic beads coupled to streptavidin at 4°C for an additional 2 hours. After washing, pellets were resuspended in Laemmli buffer. Immunoprecipitated proteins were subjected to immunoblot analysis using anti-RSK2 antibody. The experiment was repeated by loading the beads with the peptides prior to incubation with cell lysates. In addition to the routine mass spectrometry analysis performed for all peptides at the time of synthesis, the identity and the biotinylation of WT and F48A mutant peptides$_{31\text{-}51}$ present in the stock solution used for pull down experiments were confirmed by mass spectrometry.

Western Blotting and quantitation

Protein extracts, boiled for 5-10 min, were run on 8 or 10% Tris-glycine-sodium dodecyl sulfate or on 10% Tris-tricine sodium dodecyl sulfate polyacrylamide gels and transferred to polyvinylidene difluoride or nitrocellulose membranes (Immobilon; Millipore). Membranes were blocked for 1 hour with 5% milk in Tris-buffered saline (TBS), 0.1% Tween 20, incubated over-night with primary antibody in blocking reagent at the appropriate dilution, washed three times with TBS, 0.1% Tween 20, incubated 1 hour with secondary antibody diluted 2,500-10,000x in blocking reagent and washed three times with TBS, 0.1% Tween 20 and twice with TBS. Signal was detected using Pierce SuperSignal substrates. Densitometric analysis of Western blots was performed using the ImageJ software. For Li-Cor acquisition, fluorescent images were quantitated using Imagestudio.

RNA library preparation, sequencing and data analysis

Total cellular RNA was extracted from parental and RSK knockout HeLa cell lines using the method described by Chomczynski and Sacchi (8) and RNA integrity was assessed using an Agilent 2100 Bioanalyzer and 6000 RNA Pico reagents. Libraries were prepared for sequencing by Macrogen Europe using a TruSeq Stranded mRNA kit (Illumina Technologies). Library size and quantity were then verified using an Agilent

2100 Bioanalyzer coupled with DNA 1000 reagents before being sequenced on an Illumina Novaseq 6000 system. Processing of sequencing data was performed as previously described (9). Briefly, raw reads were inspected with FastQC and subjected to adapter and quality trimming by Trimmomatic version 0.39 (10). For the determination of the transcriptional expression of the RSK genes, preprocessed reads were pseudoaligned against the human transcriptome GRCh38.p12 (Ensembl release v92; accessed 22 March 2018) using kallisto (11) and transcript abundances were quantified as transcripts per million (TPM). For the identification of CRISPR/cas9-induced RSK genetic deletions, high quality reads were aligned on RSK mRNAs using Magicblast and deletions were identified using the Integrative Genomics Viewer (12). Each allele was then translated to obtain the corresponding protein product. All sequence reads were deposited in the NCBI Sequence Read Archive Database (SRA; https://www.ncbi.nlm.nih.gov/sra) and are associated with the BioProject accession number PRJNA768960.

RSK expression and CRISPR/Cas9-mutated allelic sequences are presented in supporting Dataset 2.

Alignments

Clustal Omega software (1.2.4) (13) was used to produce multiple alignments of L, ORF45, YopM as well as RSK and MSK isoforms. The following sequences were used for alignments: L (TMEV strain DA1), JX443418.1; ORF45 (KSHV strain Gk18), F5HDE4.1; YopM (Yersinia enterocolitica 8081), AF336309.1; RSK1 (RPS6KA1) (Homo sapiens), Q15418; RSK2 (RPS6KA3) (Homo sapiens), P51812; RSK2 (Rps6ka3) (Mus musculus) P18654; RSK (Corvus cornix), XP_010392786.1; RSK2 (Xenopus laevis) AAH80017.1; RSK (Danio rerio), AAI64040; RSK2 (Drosophila melanogaster), NP_523437.2; RSK (Artemia franciscana), AID60276.1; RSK (Caenorhabditis elegans), CAN86594.1; RSK3 (RPS6KA2) (Homo sapiens), Q15349; RSK4 (RPS6KA6) (Homo sapiens), Q9UK32; MSK1 (RPS6KA5) (Homo sapiens), O75582; MSK2 (RPS6KA4) (Homo sapiens), O75676.

Quantification and statistical analysis

Statistical significance was determined using two-tailed Mann-Whitney non-parametrical tests implemented in the PRISM 7 statistical analysis software (GraphPad Software, Inc., San Diego, CA). The number of independent experiments (n) and statistical comparison groups are indicated in the figures or figure legends. Asterisks denote the statistical significance of the indicated comparisons as follows: *, $p \leq 0.05$; **, $p \leq 0.01$; ***, $p \leq 0.001$

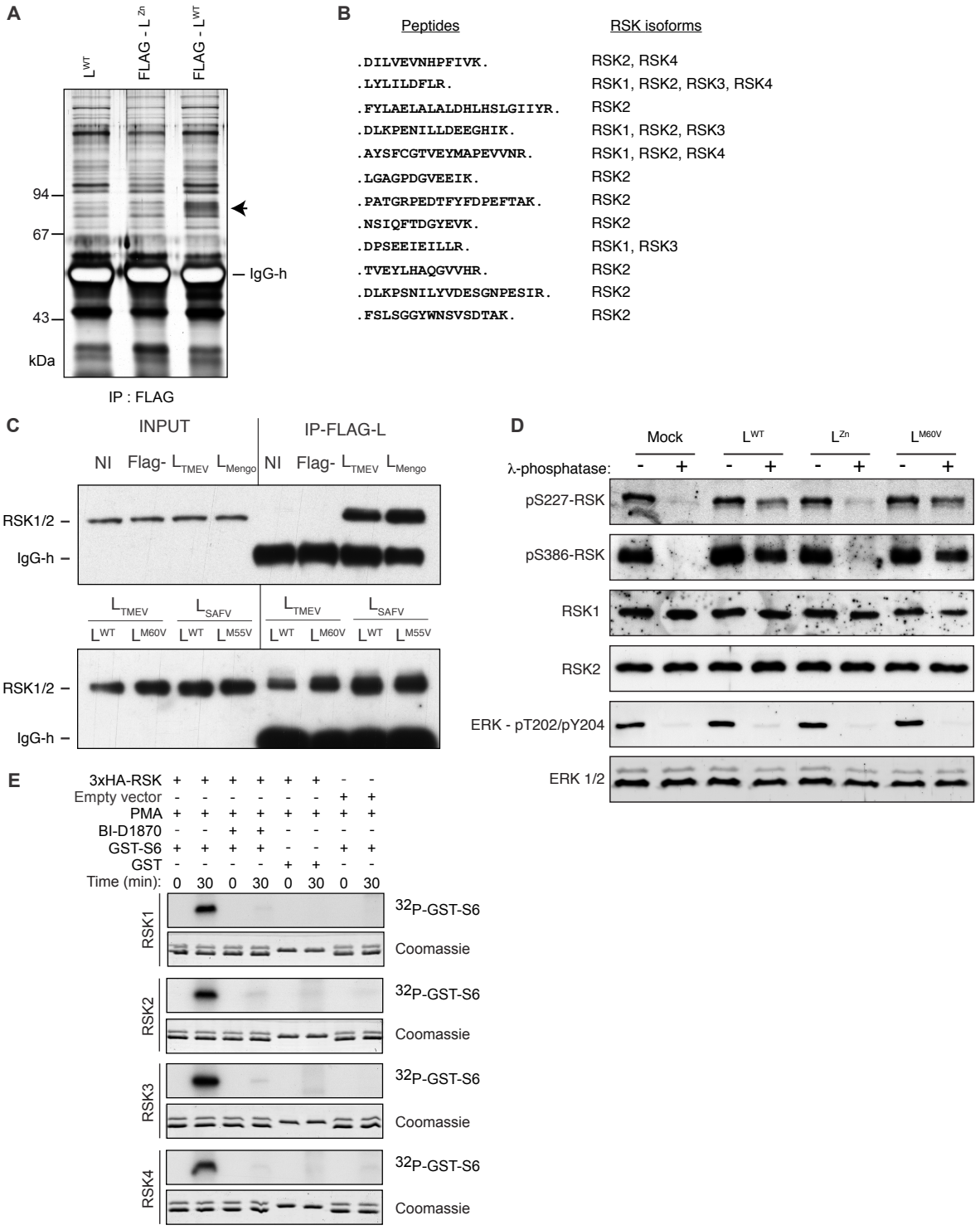

Figure S1. Identification of RSK1/2 as TMEV L binding partner which protects RSK from dephosphorylation, related to Figure 1.

(A) Silver stained SDS-PAGE of anti-FLAG immunoprecipitates from lysates of BHK-21 cells infected for 8 hours with viruses expressing untagged L^{WT}, FLAG-L^{WT} or a FLAG-tagged L protein carrying a zinc finger mutation (FLAG-L^{Zn}). The arrow points to a gel region that contained extra-density in the FLAG-L^{WT} lane, which was analyzed by mass spectrometry. IgG-h: immunoglobulin heavy chain.

(B) Peptides identified by mass spectrometry that were specific to FLAG-L^{WT} infected sample. RSK isoforms matching the identified peptide sequences are indicated.

(C) Immunoblots showing endogenous RSK1/2 proteins detected in cell lysates (left) and FLAG-L-immunoprecipitated fractions (right) of L929 cells. Upper blot: Samples from non-infected (NI) cells and from cells that were infected with untagged (FLAG-) or with FLAG-L expressing TMEV (DA1 strain) or Mengo virus (an EMCV strain). Lower blot: Samples from cells that were infected with L^{WT} and L^{M60V} variants of TMEV (DA1 strain) and with recombinant TMEV expressing L^{WT} and L^{M55V} of Saffold virus. The M60V mutation in L_{TMEV} and the corresponding M55V mutation in L_{SAFV} do not impact RSK binding. Note that although FLAG-L constructs were readily immunoprecipitated, they were not detected by immunoblots using anti-FLAG antibodies. IgG-h: immunoglobulin heavy chain.

(D) Immunoblots performed on L929 cell lysates that were either mock-treated (-) or treated with recombinant λ phosphatase (+). Samples from cells infected with viruses expressing L proteins that bind RSK2 (L^{WT} and L^{M60V}) show less dephosphorylation on RSK2 residues S227 and S386 than samples from PMA-treated mock-infected cells (Mock) or from cells infected with the mutant virus expressing L^{Zn} that lost RSK binding ability. ERK dephosphorylation (T202 and Y204) was assessed as a control for phosphatase treatment.

(E) Control kinase assays performed with the four HA-tagged RSK isoforms that were immunoprecipitated from transduced L929 cells using an anti-HA antibody. Reactions were performed using ^{32}P γ-ATP and GST-S6 fusions as RSK substrates or GST alone as control. Shown is the detection of ^{32}P-labelled-GST-S6 by autoradiography at 0 and 30 min of reaction time, and Coomassie-blue stained SDS-PAGE of reaction samples showing GST-S6 detection. Note that the lower band visible on the gels likely results from partial GST-S6 proteolysis. Kinase activity was activated using PMA and reactions were carried out with or without BI-D1870, a pan-RSK inhibitor, as indicated.

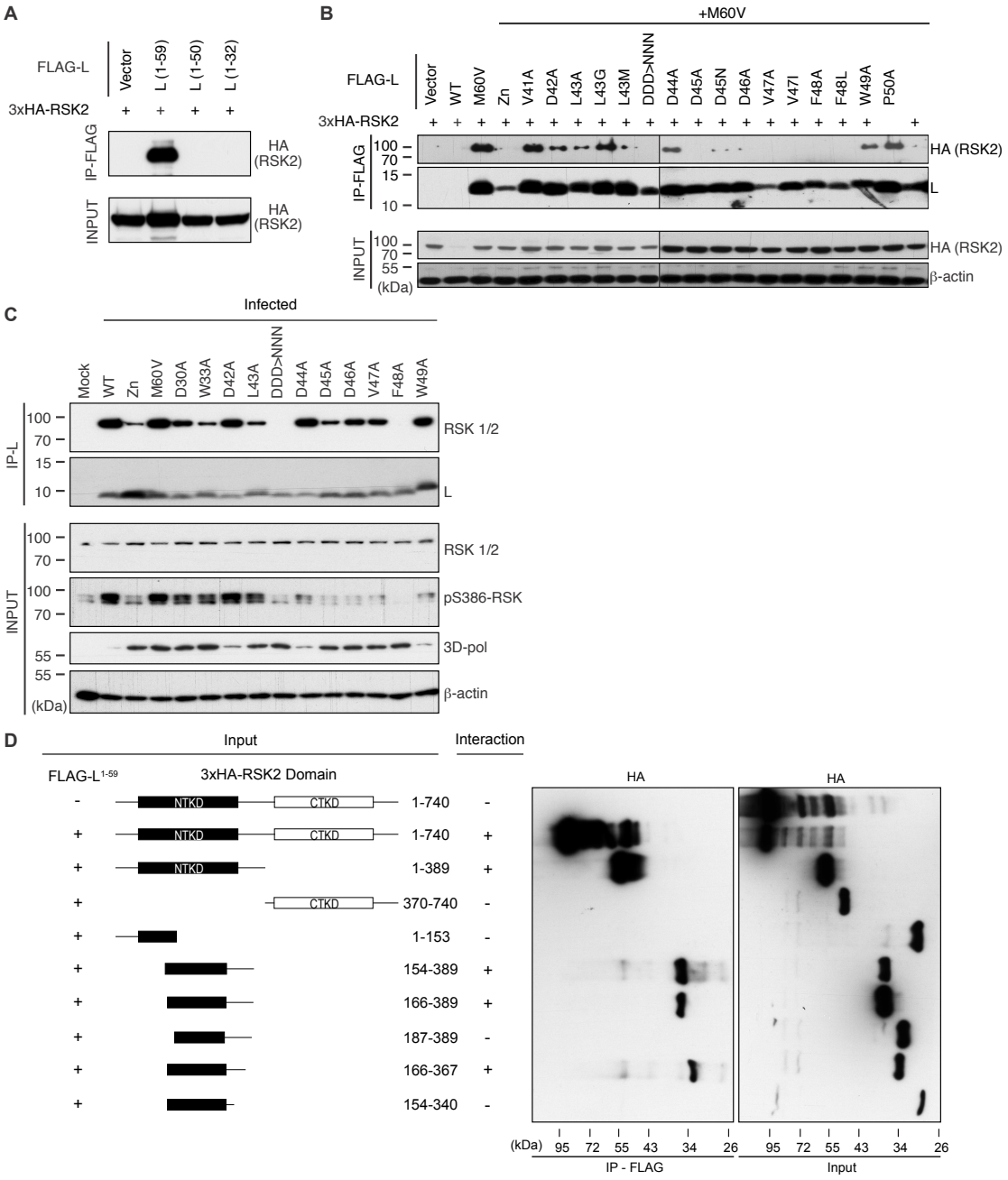

Figure S2. Mapping of the interaction between RSK and the Leader protein, related to Figure 2.

(A) Detection by immunoblot of HA (RSK2) co-immunoprecipitation with FLAG-tagged truncated L proteins from 293T cells that were co-transfected with indicated constructs.

(B) Detection by immunoblot of HA (RSK2) co-immunoprecipitation with FLAG-tagged L mutants from 293T cells co-transfected with indicated constructs. L mutations spanning the central region of L were introduced in the L^{M60V} mutant backbone because this mutant retains RSK binding ability (lane 3) and, unlike L^{WT}, does not inhibit protein expression in transfected cells. β-actin was detected as a loading control.

(C) Detection by immunoblot of endogenous RSK1/2 co-immunoprecipitation after L immunoprecipitation (anti-L antibody) from L929 cells that were infected with indicated L-mutant viruses. TMEV 3D polymerase (3D-pol) was detected in cell lysates as a control for infection. Ser386 phosphorylation (pS386) was detected as an RSK activation marker. INPUT: cell lysates; IP-FLAG: samples immunoprecipitated with anti-FLAG magnetic beads; DDD>NNN:

triple D-to-N mutation of residues 44, 45 and 46. Results are representative of four independent experiments. **(D)** Detection by immunoblot of 3xHA-RSK2 deletion mutants co-immunoprecipitation with FLAG-L^{1-59}, from 293T cells co-transfected with indicated RSK2 and L^{1-59} expressing plasmids. NTKD = amino-terminal kinase domain. CTKD = carboxy-terminal kinase domain.

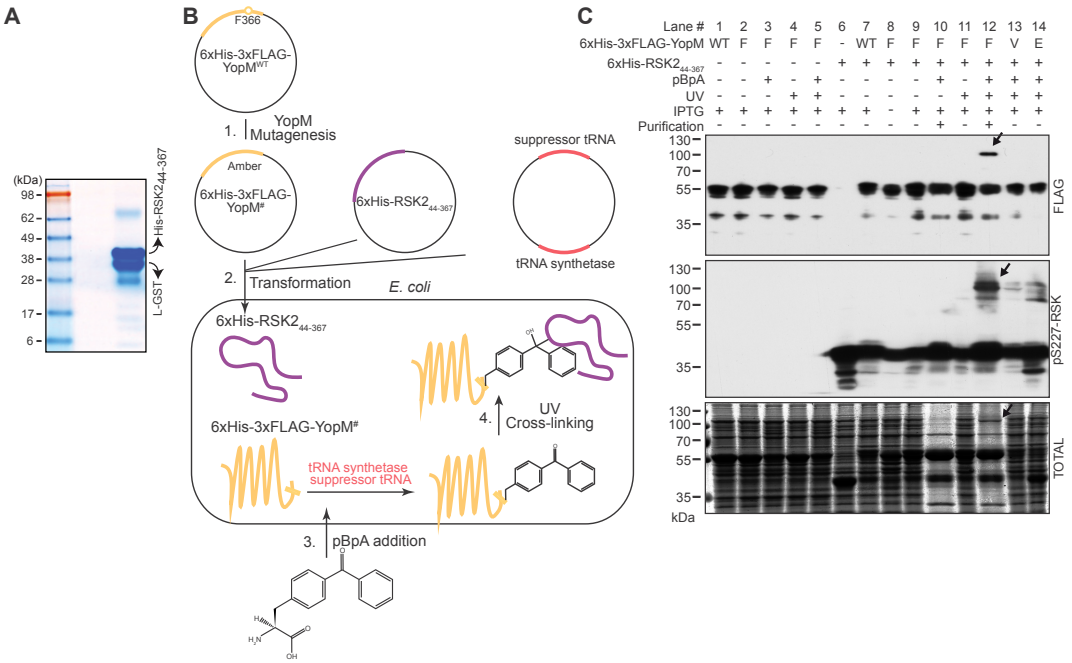
A
B
C
F366
6xHis-3xFLAG-YopM^WT
1. YopM Mutagenesis
Amber
6xHis-3xFLAG-YopM#
6xHis-RSK2 44-367
suppressor tRNA
tRNA synthetase
2. Transformation
E. coli
6xHis-RSK2 44-367
6xHis-3xFLAG-YopM#
4. UV Cross-linking
tRNA synthetase suppressor tRNA
3. pBpA addition
(kDa)
His-RSK2 44-367
L-GST
Lane # 1 2 3 4 5 6 7 8 9 10 11 12 13 14
6xHis-3xFLAG-YopM WT F F F F - WT F F F F V E
6xHis-RSK2 44-367
pBpA
UV
IPTG
Purification
FLAG
pS227-RSK
TOTAL
kDa

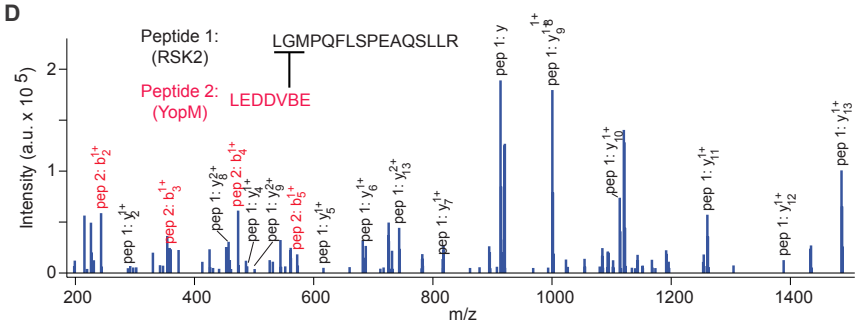
D
Peptide 1: (RSK2)
LGMPQFLSPEAQSLLR
Peptide 2: (YopM)
LEDDVBE
Intensity (a.u. x 10 5)
m/z

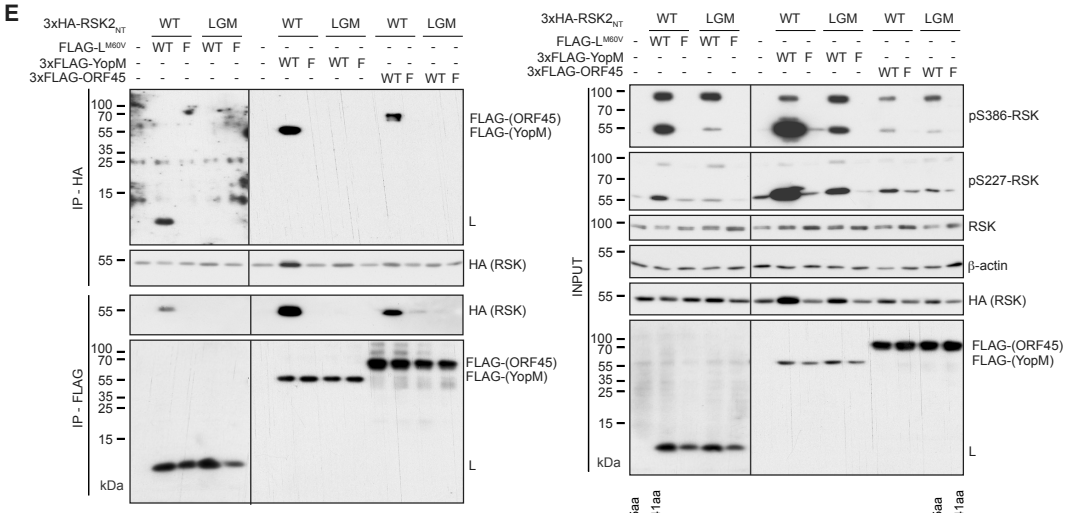
E
3xHA-RSK2 NT
WT
LGM
FLAG-L M60V
3xFLAG-YopM
3xFLAG-ORF45
IP - HA
IP - FLAG
INPUT
FLAG-(ORF45)
FLAG-(YopM)
L
HA (RSK)
pS386-RSK
pS227-RSK
RSK
β-actin
kDa

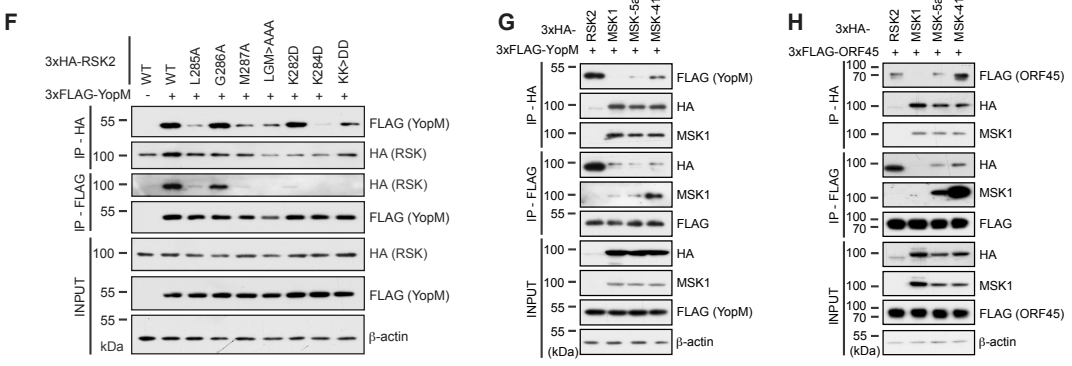
F
3xHA-RSK2
WT
L285A
G286A
M287A
LGM>AAA
K282D
K284D
KK>DD
3xFLAG-YopM
IP - HA
IP - FLAG
INPUT
FLAG (YopM)
HA (RSK)
β-actin
kDa

G
3xHA-
RSK2
MSK1
MSK-5aa
MSK-41aa
3xFLAG-YopM
IP - HA
IP - FLAG
INPUT
FLAG (YopM)
HA
MSK1
FLAG
β-actin
(kDa)

H
3xHA-
RSK2
MSK1
MSK-5aa
MSK-41aa
3xFLAG-ORF45
IP - HA
IP - FLAG
INPUT
FLAG (ORF45)
HA
MSK1
FLAG
β-actin
(kDa)

Figure S3. Identification and validation of RSK residues critical for interaction with YopM and ORF45, related to Figure 3.

(A) L:RSK2 complex formation. L and RSK2 co-elute after sequential purification of GST-tagged L and His-tagged $RSK2_{44-367}$ proteins following co-expression in *E. coli.*

(B) Principle of the cross-linking strategy. 1. YopM codons encoding F366 (or adjacent V365 and E367) residues implicated in RSK binding were mutated into an UAG amber stop codon ($YopM^{\#}$) in the 6xHis-3xFLAG-YopM bacterial expression construct. 2. Plasmids coding for 6xHis-3xFLAG-$YopM^{\#}$ and 6xHis-$RSK2_{44-367}$ were transformed into *E. coli* along with a plasmid encoding a suppressor tRNA and an aminoacyl-tRNA synthetase that loads the suppressor tRNA with the cross-linking agent pBpA. 3. Protein expression was induced with IPTG and arabinose in the presence or absence of pBpA. 4. Upon exposure to low-energy UV light ($\lambda \geq 365$nm), the benzophenone group of pBpA reacts with with otherwise unactivated carbon-hydrogen bonds (C—H) within a radius of 3 Å. Lysis of the bacteria is followed by an optional purification of the proteins of interest and mass spectrometry enables the identification of cross-linked residues.

(C) Cross-linking of $YopM^{\#}$ with $RSK_{244-367}$ in bacteria. Experimental conditions are indicated. After cross-linking, a band (arrows - lane 12) corresponding to the $YopM^{F366\#}$-RSK2 complex was detected by immunoblot with both anti-FLAG (YopM) (upper panel) and anti pS227-RSK (middle panel) antibodies. This band was absent in samples from non UV-treated bacteria (lane 10) otherwise identically processed. A similar band of lower intensity was also detected after cross-linking of $YopM^{V367\#}$ (lane 13) and $YopM^{E368\#}$ (lane 14) although these samples where not enriched for His-tagged proteins on His-TRAP columns. His-tagged proteins extracted from UV light-untreated (lane 10) and -treated bacteria (lane 12, arrow) were enriched with a His-TRAP column. The lower panel shows a Coomassie blue-stained SDS-PAGE of the samples.

(D) RSK2 peptide identified after cross-linking. The band identified with an arrow in panel B for UV-treated (lane 12) and untreated (lane 10) samples was cut, digested with trypsin and subjected to mass spectrometry. Shown is the MS2 fragmentation spectrum with assigned ion products. pBpA (B) in peptide 2 cross-linked to one or more of the three N-terminal amino acids 'LGM' of peptide 1. The cross-linked peptide was not detectable in the negative control.

(E) Representative immunoblot (n=2) showing co-immunoprecipitation of L, YopM, and ORF45, with wild type (WT) but not with KAKLGM>KAK<u>AAA</u> mutant (LGM) $RSK2^{NTKD}$, from 293T cells co-transfected with indicated constructs. Expressed L, YopM and ORF45 had either a wild type (WT) DDV<u>F</u> or a mutated (F) DDV<u>A</u> RSK-binding motif. Note that L^{M60V} mutant was used as "WT" since it readily binds RSKs and lacks toxicity in transfected cells. Phosphorylation of RSK Ser227 and Ser386 was detected as a control of RSK2 activation.
INPUT: cell lysates; IP-FLAG and IP-HA: fraction immunoprecipitated with anti-HA and anti-FLAG magnetic beads, respectively; NTKD = amino-terminal kinase domain.

(F) Mutations in the KAKLGM motif of RSK2 affect YopM binding. Plasmids expressing FLAG-YopM and indicated HA-RSK2 mutants were co-transfected in 293T cells. Co-immunoprecipitations were performed using anti-FLAG (YopM) and anti-HA (RSK2) antibodies. Shown is a representative experiment (n=3) detecting HA and FLAG in cell lysates (INPUT) and immunoprecipitated (IP) fractions.

(G-H) Representative immunoblots (n=4) showing co-immunoprecipitation of 3xFLAG-YopM **(F)** and 3xFLAG-ORF45 **(G)** with MSK1 chimeras carrying the (K)AKLGM motif of RSK2. Co-immunoprecipitations were carried out from 293T cells co-transfected with plasmids expressing FLAG-tagged YopM or ORF45 and

constructs expressing 3xHA-tagged RSK2, MSK1 or MSK1 chimeras carrying 5 (MSK1-5aa) or 41 (MSK1-41aa) RSK2 residues encompassing the (K)AKLGM sequence. INPUT: cell lysates; IP-FLAG and IP-HA; fractions immunoprecipitated with anti-FLAG and anti-HA magnetic beads respectively.

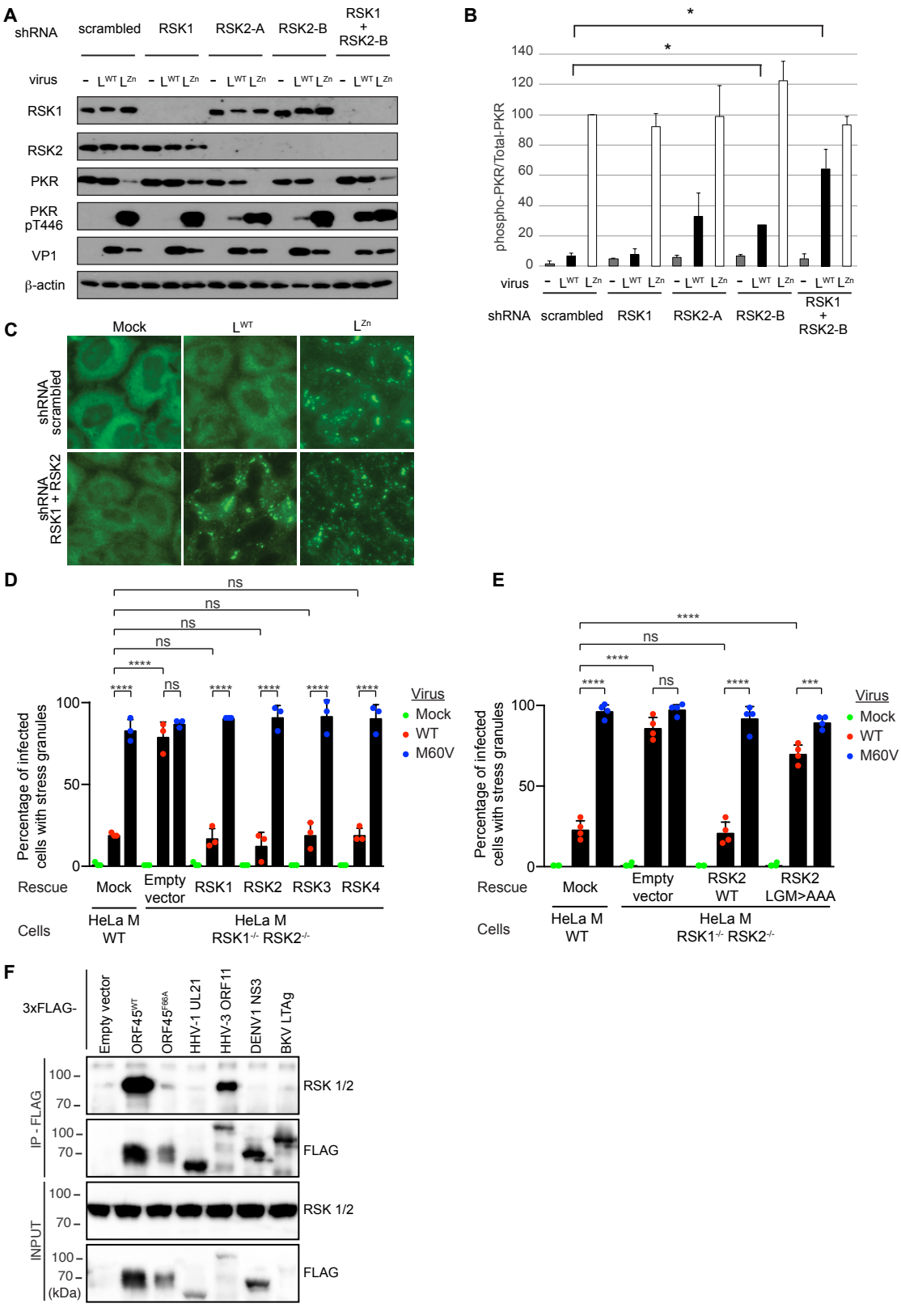

Figure S4. PKR activation inhibition by L is dependent on RSK1 and 2, related to Figure 4.

(A) Immunoblots showing the extent of PKR activation (phospho-Thr446: pT446) in infected HeLa-M cells knocked down for RSK1/2 expression. HeLa-M cells transduced for 48h with lentiviral constructs expressing scrambled shRNA or shRNA directed against HuRSK1, HuRSK2 or a combination thereof were either mock-infected (-) or infected for 12 hours with TMEV expressing either WT (L^{WT}) or zinc-finger mutant

(L^{Zn}) L proteins. RSK1 and RSK2 were detected to confirm efficient knock-down. Viral VP1 capsid protein was detected as a control of infection and β-actin was detected as loading control.

(B) Quantification of PKR phosphorylation. Graphs show the mean +/- SD of the pT446-PKR/total PKR ratio obtained by quantification of bands on immunoblots from three independent experiments. Values were compared to those of non-infected cells. * $p<0.05$ in a one-tailed Mann-Whitney test.

(C) Stress granule detection by eIF3 immunolabeling in HeLa-M cells infected for 10h as indicated. Three days prior to infection, cells were transduced with lentiviral vectors derived from pLKO.1 and expressing either a control (scrambled) shRNA or a combination of shRNAs targeting RSK1 and RSK2.

D) Functional importance of individual RSK genes for the inhibition of stress granule assembly by the TMEV leader protein. Bar graph showing the percentage of infected cells with stress granules in mock-infected or infected HeLa M cells. $RSK1^{-/-}$ $RSK2^{-/-}$ double knockout HeLa M rescued with an empty vector or with the same vector expressing the individual human RSK genes were either mock-infected or infected with 5PFU/cell of KJ6 derivatives expressing either L^{WT} or L^{M60V}. Twelve hours post-infection, cells were processed for eiF3 (stress granules) and TMEV 3D polymerase (virus) immunostaining and the number of stress granule positive cells relative to 3D-positive cells were counted and expressed as percentages.

(E) As above with the exception that $RSK1^{-/-}$ $RSK2^{-/-}$ double knockout HeLa M cells were recued with a RSK2 LGM>AAA mutant instead of RSK genes.

(F) Detection by immunoblot of endogenous RSK1/2 co-immunoprecipitation after FLAG immunoprecipitation from 293T cells transfected with indicated constructs. WT and F66A mutant ORF45 were used as positive and negative controls, respectively. INPUT: cell lysates; IP-FLAG: samples immunoprecipitated with anti-FLAG magnetic beads.

Table S1. Table of plasmid constructs used in this study.

Eukaryotic expression vectors (L, YopM and ORF45)			
Name	**Tag**	**Encoded protein, particularity**	**Type (parental)**
pFS199	N-term Flag	Empty	pcDNA3
pFS204	N-term Flag	Flag-L_{DA} (WT), L from TMEV strain DA	pcDNA3
pFS207	N-term Flag	Flag-L_{DA} (1-59), truncated L	pcDNA3
pFS219	N-term Flag	Flag-L_{DA} (1-50), truncated L	pcDNA3
pFS211	N-term Flag	Flag-L_{DA} (1-32), truncated L	pcDNA3
pFS209	N-term Flag	Flag-L_{GDVII} (WT), L of TMEV strain GDVII	pcDNA3
pFS200	N-term Flag	Flag-L_{SAFV} (WT), L from SAFV2	pcDNA3
pTM624		eGFP	pcDNA3
pTM996	N-term 3xFlag	$Prom_{CMV}$-3xFlag-Empty / Gateway cassette	pcDNA3
pTM1004	N-term 3xFlag	$Prom_{CMV}$-3xFlag-L_{DA}, WT L of strain DA	pcDNA3
pTM1055	N-term 3xFlag	$Prom_{CMV}$-3xFlag-L_{DA}, F48A L_{DA} mutant	pcDNA3
pTM1056	N-term 3xFlag	$Prom_{CMV}$-3xFlag-L_{DA}, M60V L_{DA} mutant	pcDNA3
pGDB07	N-term 3xFlag	3xFlag-ORF45 (KSHV)	pTM996
pGDB08	N-term 3xFlag	3xFlag-$ORF45_{F36A}$ (F36A mutant ORF45)	pTM996
pTM1005	N-term 3xFlag	3xFlag-YopM (*Y.enterocolitica* W22703)	pTM996
pTM1020	N-term 3xFlag	3xFlag-$YopM_{F366A}$ (F366A mutant YopM)	pTM996
pTM1021	N-term 3xFlag		pTM1021
pMiP32	N-term Flag	Flag-L^{M60V}-(IRES)-GFP, M60V mutant	pcDNA3
pMIP68	N-term 3xFlag	3xFlag-$L^{M60V+Zn}$-(IRES)-GFP, M60V mutant	pcDNA3
pMIP70	N-term 3xFlag	3xFlag-$L^{M60V+DDD>NNN}$-(IRES)-GFP, DDD mut.	pcDNA3
pMIP92	N-term 3xFlag	3xFlag-$L^{M60V+V41A}$-(IRES)-GFP, V41A+M60V	pcDNA3
pMIP93	N-term 3xFlag	3xFlag-$L^{M60V+D42A}$-(IRES)-GFP, D42A+M60V	pcDNA3
pMIP94	N-term 3xFlag	3xFlag-$L^{M60V+L43A}$-(IRES)-GFP, L43A+M60V	pcDNA3
pMIP95	N-term 3xFlag	3xFlag-$L^{M60V+L43G}$-(IRES)-GFP, L43G+M60V	pcDNA3
pMIP96	N-term 3xFlag	3xFlag-$L^{M60V+L43M}$-(IRES)-GFP, L43M+M60V	pcDNA3
pMIP97	N-term 3xFlag	3xFlag-$L^{M60V+D44A}$-(IRES)-GFP, D44A+M60V	pcDNA3
pMIP98	N-term 3xFlag	3xFlag-$L^{M60V+D45A}$-(IRES)-GFP, D45A+M60V	pcDNA3
pMIP99	N-term 3xFlag	3xFlag-$L^{M60V+D45N}$-(IRES)-GFP, D45N+M60V	pcDNA3
pMIP100	N-term 3xFlag	3xFlag-$L^{M60V+D46A}$-(IRES)-GFP, D46A+M60V	pcDNA3
pMIP101	N-term 3xFlag	3xFlag-$L^{M60V+V47A}$-(IRES)-GFP, V47A+M60V	pcDNA3
pMIP102	N-term 3xFlag	3xFlag-$L^{M60V+V47I}$-(IRES)-GFP, V47I+M60V	pcDNA3
pMIP103	N-term 3xFlag	3xFlag-$L^{M60V+F48A}$-(IRES)-GFP, F48A+M60V	pcDNA3
pMIP104	N-term 3xFlag	3xFlag-$L^{M60V+F48L}$-(IRES)-GFP, F48L+M60V	pcDNA3
pMIP105	N-term 3xFlag	3xFlag-$L^{M60V+W49A}$-(IRES)-GFP, W49A+M60V	pcDNA3
pMIP106	N-term 3xFlag	3xFlag-$L^{M60V+P50A}$-(IRES)-GFP, P50A+M60V	pcDNA3

Eukaryotic expression vectors (RSK)			
Name	**Tag**	**Encoded protein, particularity**	Type (parental)
pFS217	N-term 3xHA	Empty $Prom_{PGK}$-3xHA-IRES-Neo	Lentiviral (pTM898)
pFS221	N-term 3xHA	$Prom_{PGK}$-3xHA-MuRSK1-IRES-Neo	Lentiviral (pTM898)
pFS222	N-term 3xHA	$Prom_{PGK}$-3xHA-MuRSK2-IRES-Neo	Lentiviral (pTM898)
pFS226	N-term 3xHA	$Prom_{PGK}$-3xHA-MuRSK3-IRES-Neo	Lentiviral (pTM898)
pFS227	N-term 3xHA	$Prom_{PGK}$-3xHA-MuRSK4-IRES-Neo	Lentiviral (pTM898)
pFS223	N-term 3xHA	$Prom_{PGK}$-3xHA-$MuRSK2_{1-389}$-IRES-Neo	Lentiviral (pTM898)
pFS224	N-term 3xHA	$Prom_{PGK}$-3xHA-$MuRSK2_{370-740}$-IRES-Neo	Lentiviral (pTM898)

pFS241	N-term 3xHA	$Prom_{PGK}$-3xHA-$MuRSK2_{1-153}$-IRES-Neo	Lentiviral (pTM898)
pFS243	N-term 3xHA	$Prom_{PGK}$-3xHA-$MuRSK2_{154-389}$-IRES-Neo	Lentiviral (pTM898)
pFS253	N-term 3xHA	$Prom_{PGK}$-3xHA-$MuRSK2_{187-340}$-IRES-Neo	Lentiviral (pTM898)
pFS256	N-term 3xHA	$Prom_{PGK}$-3xHA-$MuRSK2_{154-340}$-IRES-Neo	Lentiviral (pTM898)
pFS257	N-term 3xHA	$Prom_{PGK}$-3xHA-$MuRSK2_{166-389}$-IRES-Neo	Lentiviral (pTM898)
pFS258	N-term 3xHA	$Prom_{PGK}$-3xHA-$MuRSK2_{187-389}$-IRES-Neo	Lentiviral (pTM898)
pFS260	N-term 3xHA	$Prom_{PGK}$-3xHA-$MuRSK2_{166-367}$-IRES-Neo	Lentiviral (pTM898)
pTM952		$Prom_{CMV}$-Empty-IRES-neo	Lentiviral (pCCLsin)
pTM1082		$Prom_{CMV}$-MuRSK2-IRES-neo	Lentiviral (pTM952)
pMIP130	N-term 3xHA	$muRSK2_{1-389}$	Lentiviral (pFS223)
pMIP204	N-term 3xHA	$muRSK2_{1-389}$ (LGM>AAA) mutant of pMIP130	Lentiviral (pFS223)
pFS236	N-term 3xHA	$Prom_{PGK}$-3xHA-MuRSK2-IRES-Hygro	Retroviral (pQCXIH)
pMIP206	N-term 3xHA	MuRSK2 (G286A) mutant of pFS236	Retroviral (pQCXIH)
pMIP207	N-term 3xHA	MuRSK2 (M287A) mutant of pFS236	Retroviral (pQCXIH)
pMIP208	N-term 3xHA	MuRSK2 (LGM>AAA) mutant of pFS236	Retroviral (pQCXIH)
pMIP209	N-term 3xHA	MuRSK2 (K282D) mutant of pFS236	Retroviral (pQCXIH)
pMIP210	N-term 3xHA	MuRSK2 (K284D) mutant of pFS236	Retroviral (pQCXIH)
pMIP211	N-term 3xHA	MuRSK2 (KK>DD) mutant of pFS236	Retroviral (pQCXIH)
pcDNA4	N-term HA	$Prom_{CMV}$-HA-HuMSK1	pcDNA4
pMIP223	N-term HA	$Prom_{CMV}$-HA-HuMSK1/RSK2 (5aa chimera)	pcDNA4
pMIP224	N-term HA	$Prom_{CMV}$-HA-HuMSK1/RSK2 45aa chimera)	pcDNA4

Bacterial expression vectors			
Name	**Tag**	**Encoded protein, particularity**	Type (parental)
pMIP188	6xHis-3xFlag	$Prom_{T7}$ 6xHis-3xFlag -YopM	pET-15b
pMIP189	6xHis-3xFlag	$Prom_{T7}$ 6xHis-3xFlag –YopM (V365->amber)	pET-15b
pMIP190	6xHis-3xFlag	$Prom_{T7}$ 6xHis-3xFlag –YopM (F366->amber)	pET-15b
pMIP191	6xHis-3xFlag	$Prom_{T7}$ 6xHis-3xFlag –YopM (E367->amber)	pET-15b
pMIP192	6xHis	$Prom_{T7}$ 6xHis-$MuRSK2_{44-367}$	pRSFDUET
pEVOL			pEVOL

Viruses (recombinant TMEV)			
Name	**Tag**	**Encoded protein, particularity**	Type (parental)
KJ6	/	L_{DA} (WT), L929 cell-adapted capsid	TMEV (DA1)
TM659	/	L_{DA} (Zn), zinc finger L mutant	TMEV (KJ6)
FB09	/	L_{DA} (M60V), Theilodomain mutant L	TMEV (KJ6)
TM1017	N-term 3xFLAG	3xFlag_L_{DA}, L (WT) from TMEV strain DA	TMEV (KJ6)
TM1031	N-term 3xFLAG	3xFlag_L_{Mengo}, L (WT) from Mengo virus	TMEV (KJ6)
TM1033	N-term 3xFLAG	3xFlag_L_{SAFV}, L (WT) from SAFV	TMEV (KJ6)
TM1034	N-term 3xFLAG	3xFlag_L_{SAFV} (M55V) L mutant of TM1033	TMEV (KJ6)
SD18	N-term Flag	Flag-L_{DA}, WT L from TMEV strain DA	TMEV (KJ6)
SD22	N-term Flag	Flag-L_{DA}^{Zn}, L^{Zn} mutant TMEV strain DA	TMEV (KJ6)
FS269	N-term Flag	Flag-L_{Mengo} (WT), L from Mengo virus	Mengo virus
MIP124	/	L_{DA} (WT), stop codon in L* ORF	TMEV (KJ6)
MIP125	/	L_{DA} (Zn), Zn L mutant of MIP124	TMEV (KJ6)
MIP126	/	L_{DA} (M6V), M60V L mutant of MIP124	TMEV (KJ6)
MIP137	/	L_{DA} (D30A), D30A L mutant of MIP124	TMEV (KJ6)
MIP138	/	L_{DA} (W33A), W33A L mutant of MIP124	TMEV (KJ6)
MIP139	/	L_{DA} (D42A), D42A L mutant of MIP124	TMEV (KJ6)

MIP140	/	L_{DA} (L43A), L43A L mutant of MIP124	TMEV (KJ6)
MIP141	/	L_{DA} (DDD-NNN), triple mutant of MIP124	TMEV (KJ6)
MIP142	/	L_{DA} (D44A), D44A L mutant of MIP124	TMEV (KJ6)
MIP143	/	L_{DA} (D45A), D45A L mutant of MIP124	TMEV (KJ6)
MIP144	/	L_{DA} (D46A), D46A L mutant of MIP124	TMEV (KJ6)
MIP145	/	L_{DA} (V47A), V47A L mutant of MIP124	TMEV (KJ6)
MIP146	/	L_{DA} (F48A), F48A L mutant of MIP124	TMEV (KJ6)
MIP147	/	L_{DA} (W49A), W49A L mutant of MIP124	TMEV (KJ6)

shRNA	**(lentiviral)**		
Name		**Encoded RNA, particularity**	Type (parental)
pYH37	/	shRNA targeting HuRSK1	Lentiviral (pLKO.1)
pYH39	/	shRNA targeting HuRSK2 (clone A)	Lentiviral (pLKO.1)
pYH40	/	shRNA targeting HuRSK1 (clone B)	Lentiviral (pLKO.1)

Name		**Encoded RNA, particularity**	Type (parental)
pYH47	/	sgRNA targeting HuRSK2 guide 1	pX461
pYH48	/	sgRNA targeting HuRSK2 guide 2	pX461
pTM1077	/	sgRNA targeting HuRSK1 guide 1	pX461
pTM1079	/	sgRNA targeting HuRSK1 guide 2	pX461

SI References

1. R. B. DuBridge, *et al.*, Analysis of mutation in human cells by using an Epstein-Barr virus shuttle system. *Mol. Cell. Biol.* **7**, 379–387 (1987).
2. B. Dong, M. Niwa, P. Walter, R. H. Silverman, Basis for regulated RNA cleavage by functional analysis of RNase L and Ire1p. *RNA* **7**, 361–373 (2001).
3. F. A. Ran, *et al.*, Genome engineering using the CRISPR-Cas9 system. *Nat. Protoc.* **8**, 2281–2308 (2013).
4. J. Moffat, *et al.*, A lentiviral RNAi library for human and mouse genes applied to an arrayed viral high-content screen. *Cell* **124**, 1283–1298 (2006).
5. A. Follenzi, L. E. Ailles, S. Bakovic, M. Geuna, L. Naldini, Gene transfer by lentiviral vectors is limited by nuclear translocation and rescued by HIV-1 pol sequences. *Nat Genet* **25**, 217–222 (2000).
6. K. Jnaoui, T. Michiels, Adaptation of Theiler's virus to L929 cells: Mutations in the putative receptor binding site on the capsid map to neutralization sites and modulate viral persistence. *Virology* **244** (1998).
7. G. M. Duke, A. C. Palmenberg, Cloning and synthesis of infectious cardiovirus RNAs containing short, discrete poly(C) tracts. *J. Virol.* **63** (1989).
8. P. Chomczynski, N. Sacchi, Single-step method of RNA isolation by acid guanidinium thiocyanate-phenol-chloroform extraction. *Anal. Biochem.* **162**, 156–159 (1987).
9. M. Hosmillo, *et al.*, Norovirus Replication in Human Intestinal Epithelial Cells Is Restricted by the Interferon-Induced JAK/STAT Signaling Pathway and RNA Polymerase II-Mediated Transcriptional Responses. *MBio* **11** (2020).
10. A. M. Bolger, M. Lohse, B. Usadel, Trimmomatic: a flexible trimmer for Illumina sequence data. *Bioinformatics* **30**, 2114–2120 (2014).
11. N. L. Bray, H. Pimentel, P. Melsted, L. Pachter, Near-optimal probabilistic RNA-seq quantification. *Nat. Biotechnol.* **34**, 525–527 (2016).
12. J. T. Robinson, *et al.*, Integrative genomics viewer. *Nat. Biotechnol.* **29**, 24–26 (2011).
13. M. Goujon, *et al.*, A new bioinformatics analysis tools framework at EMBL-EBI. *Nucleic Acids Res* **38**, W695-9 (2010).